

## Inversion of Transient Hydraulic Head Variation Caused by a Controlled Point Source

*Dorte Dam, Niels B. Christensen and Kurt I. Sørensen*

Department of Earth Sciences, University of Aarhus, Denmark

### Introduction

An increasing need for surveillance of the quality of our ground water resources requires a comprehensive hydraulic modeling. A thorough knowledge of the hydraulic parameters is a necessity for reliable hydraulic modeling. Pumping and slug tests have usually been the main source of information about the hydraulic conductivity and the specific storage. Pumping tests result in conductivities and storage coefficients averaged over large volumes, and slug tests are often seriously affected by the well screens and filter packs.

A new method for in situ determination of the hydraulic conductivity and the specific storage has been developed at the University of Aarhus. By making use of a hollow auger drill stem it is possible to inject water directly into the formation and measure the rise in hydraulic head at a short distance from the injection point. Other procedures for in situ determination of hydraulic parameters have been developed (Fejes and J6sa, 1990).

The measured data (the transient hydraulic head variations) are interpreted using an inversion algorithm based on a least squares iterative formalism. To make the problem more linear the inversion is carried out in the log parameter space. The model response applied is the transient head variations due to a point source in a homogenous isotropic fullspace, where the source is considered as a step source. Since there are only three model parameters to be estimated and typically more than one hundred data, the inverse problem is strongly overdetermined.

### The forward problem

The solution to the 3-D differential equation of flow in a homogeneous isotropic aquifer with appropriate initial and boundary condition is given by Carslaw and Jaeger (1959).

$$\phi(t,r) = \frac{Q}{4\pi Kr} \operatorname{erfc}\left(r\sqrt{\frac{S}{4Kt}}\right) + H = \frac{Q}{4\pi Kr} \operatorname{erfc}\left(\sqrt{\frac{u}{t}}\right) + H \quad (1)$$

- $\phi$  : change in potential head (m)
- $Q$  : water injection rate ( $\text{m}^3 \text{ s}^{-1}$ )
- $K$  : hydraulic conductivity ( $\text{m s}^{-1}$ )
- $S$  : specific storage ( $\text{m}^{-1}$ )
- $r$  : radial distance from the injection point (m)
- $t$  : time since injection start (s)
- $H$  : initial head (m)
- $u$  : characteristic time constant,  $u = Sr^2/4K$  (s)

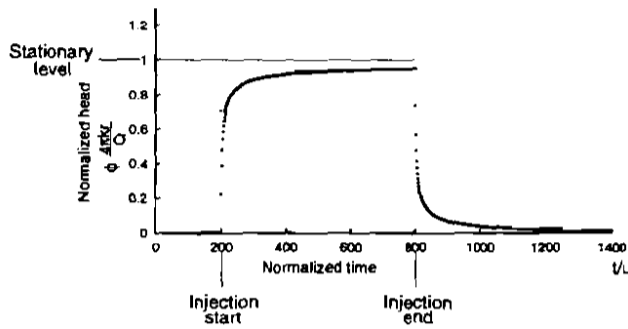


Fig. 1. The theoretical curve, when  $K = 3 \cdot 10^{-3} \text{ m/s}$ ,  $S = 3 \cdot 10^{-3} \text{ m}^{-1}$ ,  $r = 1 \text{ m}$  and  $Q = 3 \cdot 10^{-4} \text{ m}^3/\text{s}$ , which gives a characteristic time constant,  $u = Sr^2/4K = 1/4$  seconds. The injection is turned on after 200 time constants and switched off after another 600 time constants.

### Inversion

The task is to estimate the hydraulic conductivity and the specific storage from a time series of typically more than 300-700 observations. The least squares inverse formalism applied is presented below (Tarantola and Valette, 1982; Jacobsen, 1993; Nielsen, 1992):

$$m_{n+1}^{est} = (G_n^T C_d^{-1} G_n)^{-1} G_n^T C_d^{-1} (d - g(m_n^{est})) + m_n^{est} \quad (2)$$

- $d$  : measured data values (dimension N)
- $C_d$  : measured data covariances (dimension  $N \times N$ )
- $m_{n+1}^{est}$  : improved parameter estimate (dimension M)
- $m_n^{est}$  : previous parameter estimate (dimension M)
- $G_n$  : the Jacobian matrix at  $m = m_n$  (dimension  $N \times M$ )
- $g(\cdot)$  : non-linear data-parameter relationship:  $\phi = g(m)$

To make the problem more linear the variables  $K$ , and  $S$  are changed to  $\log_e(K)$  and  $\log_e(S)$  (eq. 3). Misjudgment of the initial head will introduce a bias on all data and result in inconsistency with the model. To overcome this problem the initial head

was included in the model parameter space, and as a secondary profit this also minimizes the data processing before inversion. As it will appear later the initial head is well determined, and it is not very correlated neither to S nor to K.

$$G_n = \begin{bmatrix} \frac{\partial \phi_1}{\partial \ln k} & \frac{\partial \phi_1}{\partial \ln s} & \frac{\partial \phi_1}{\partial H} \\ \cdot & \cdot & \cdot \\ \cdot & \cdot & \cdot \\ \frac{\partial \phi_n}{\partial \ln k} & \frac{\partial \phi_n}{\partial \ln s} & \frac{\partial \phi_n}{\partial H} \end{bmatrix} = \begin{bmatrix} \frac{\partial \phi_1}{\partial \ln k} & \frac{\partial \phi_1}{\partial \ln s} & 1 \\ \cdot & \cdot & \cdot \\ \cdot & \cdot & \cdot \\ \frac{\partial \phi_n}{\partial \ln k} & \frac{\partial \phi_n}{\partial \ln s} & 1 \end{bmatrix} \quad (3)$$

When the effect of the non-linearity is not too severe, the inversion will converge to the same solution, independent of initial guess. When non-linearity is significant, secondary minima or maxima may exist. To get an impression of the error surface iterations can be started with a variety of initial guesses (Menke, 1989; Tarantola and Valette, 1982; Nielsen, 1992). In the case of a parameter space consisting of only two parameters,  $\log_e(S)$  and  $\log_e(K)$  the error surface can be directly mapped (Charles et al., 1989). This analysis gives no indication of ambiguity concerning the least squares solution.

For the purely overdetermined linear problem the matrix of posterior parameter covariances  $C_m$  can be obtained by:

$$C_m = (G^T C_d^{-1} G)^{-1} \quad (4)$$

For simplicity the data errors are assumed not to be correlated i.e. the data covariance matrix is diagonal and the posterior parameter covariances matrix,  $C_m$  can then be described by:

$$C_m = (G^T \sigma_d^{-2} I G)^{-1} \quad (5)$$

where  $\sigma_d$  is the data standard deviation. If  $g(m)$  is only weakly non-linear the posterior covariance matrix,  $C_m$  for the overdetermined non-linear problem is well approximated through eq. 4 respectively eq. 5, (Jacobsen, 1992).

### Analysis of the inverse problem

The standard deviation of the various model parameters as a function of model parameters K and S has been examined (fig. 2). The length of the time series, the sample density, the injection rate, and the standard deviation of data are fixed at values relevant to the present design of the tool.

The surfaces in figure 2 present the analysis of the response from various choices of S and K. The length of the time series is  $2 \times 120 + 10$  seconds, i.e. 10 seconds before the source is turned on, 120 seconds after the source is turned on, and

another 120 seconds after the source is switched off. The source is considered as a step source with a constant injection of  $3 \cdot 10^{-4} \text{ m}^3/\text{s}$ , the radial distance from the source is 1 m and the absolute standard deviation on data is 1.5 mm.

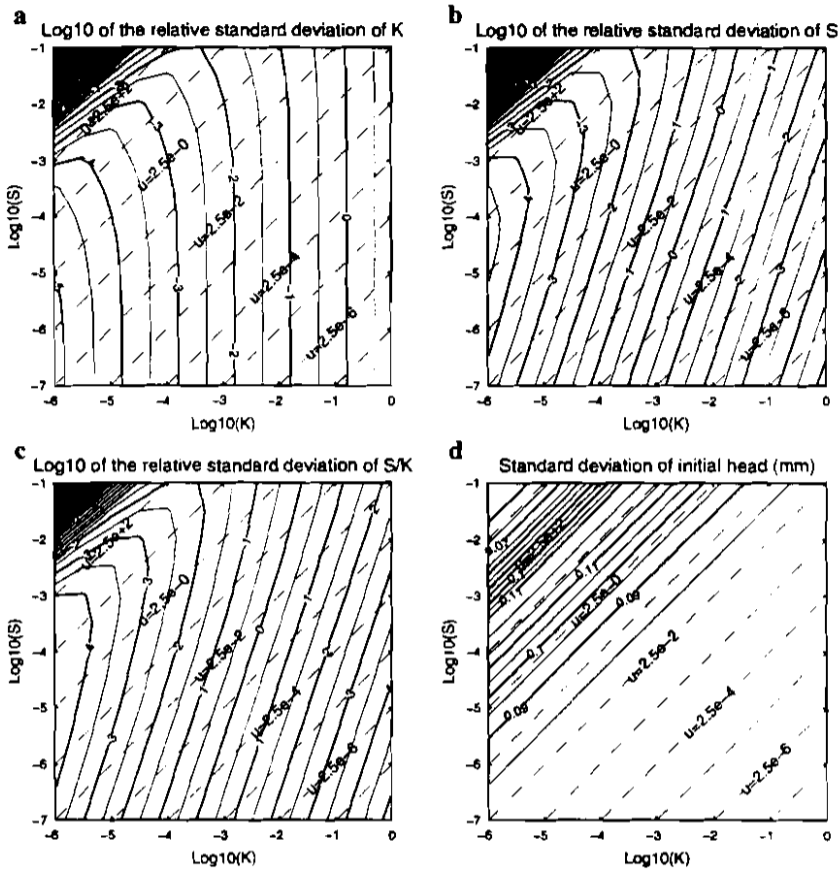


**Fig. 2.** Standard deviation of the model parameters as a function of model parameters K (hydraulic conductivity) and S (specific storage). The length of the time series is fixed at  $2 \times 120 + 10$  seconds with a sample density of 3 samples per second, the injection is  $3 \cdot 10^{-4} \text{ m}^3/\text{s}$  and the standard deviation of data is 1.5 mm. The dashed lines are lines of equal characteristic time constants,  $u$ . a the relative standard deviation of K, b the relative standard deviation of S, c the relative standard deviation of S/K, and d the standard deviation of the initial head.

The corresponding analysis of the response from a time series of 120 seconds, solely for the increasing part of the response, from 10 seconds before turn-on and 120 seconds after, or from the decreasing part of the response after the source is turned off, differ mainly at the general level of the surfaces increased by a factor of  $\sqrt{2}$  compared to the analysis of the response from the time series of  $2 \times 120$  seconds.

The level of the standard deviation surfaces depends partly on the standard deviation of data,  $\sigma_d$ , partly on the injection,  $Q$ . The relative standard deviations are inversely proportional to  $Q$  and directly proportional to  $\sigma_d$ .

For characteristic time constants,  $u$  (eq. 1), less than approximately 2.5 seconds, the standard deviation of  $K$  depends solely on  $K$  (fig. 2a), and the surface of the relative standard deviation of  $K$  slopes with a gradient of approximately 1. This shows that the data noise is dominating. The hydraulic head is inverse proportional to  $K$ , when stationary conditions are achieved (cf. eq. 1:  $\phi(\infty, r) = Q/4\pi K r$ ). Therefore, assuming absolute noise on data, an increase in  $K$ -values causes an increase in the relative standard deviation of the model parameters.

The standard deviation of  $S$  and  $S/K$  depends on  $K$  and  $S$ , independent of characteristic time constant. The standard deviation of  $S$  and  $S/K$  decreases with increasing  $S$ -values. The surface of the relative standard deviation of  $S$  slopes with a gradient larger than 1. Besides the above-mentioned effect of the data noise, the information about  $S$  also diminishes because the stationary level is reached faster when the  $K$ -value increases (i.e. less time and fewer samples in the early stage).

When the  $K$ -value is small and the  $S$ -value large, neither  $K$ ,  $S$  nor  $S/K$  are determined. When the time constant,  $u$ , exceeds approximately 1000 seconds,  $K$ ,  $S$ , and  $S/K$  are completely undetermined. Large  $S$ -values result in a smooth response curve, and small  $K$ -values find expression in a high amplitude. This means that the stationary level is never reached.

The direction of the ravine in the surfaces of relative standard deviation of  $K$ ,  $S$ , and  $S/K$  corresponds to a characteristic time constant of approximately 0.25 seconds or a length of the time series of 1000 time constants (fig. 2a-c). This implies that the location of the ravine is dependent on the length of the time series. The longer time series - the longer towards the upper-left corner the ravine is located.

### Experimental Design

For a given demand on the maximum standard deviation of a model parameter it is possible by means of figure 3a-d to find the required length of the time series and the required number of samples per time constant.

It is not surprising to notice that the standard deviation of  $K$  decreases by approximately  $\sqrt{N}$ , where  $N$  is the number of samples, as the sample density increases (corresponding to decreasing time interval between samples), or as the length of the time series increases (fig. 3a).

Likewise, the standard deviation of  $S$  and  $S/K$  diminishes as the sample density increases, but the decrease in the standard deviation of  $S$  and  $S/K$  is not as pronounced for increasing length of time series as in the case of the standard deviation of  $K$  (fig. 3b and 3c). When the time series is longer than 200 time constants ( $\log_{10}(t/u) \sim 2.3$ ), the contours are approximately vertical. This implies

that the certainty of the determination of the model parameters,  $S$  and  $S/K$  is not improved notably by further sampling in time. As we would expect, the information about the  $S$ - or  $S/K$ -parameter lies at the early times, just after the source is turned on, or just after it is turned off. Comparing figure 3b and 3c it is seen that, for short timeseries,  $S$  alone is better determined than the fraction  $S/K$ .

At all times, except for time series shorter than the time between samples, the initial head is determined at least with the certainty of the data, which is 1.5 mm (fig. 3d). The standard deviation of the initial head also decreases as the sample density and time series length increases. An increase in time series length results in more measurements of the last part of the response (cf. fig. 1  $t/u \approx 1200-1400$ ) and hence more measurements of the model parameter we wish to determine.

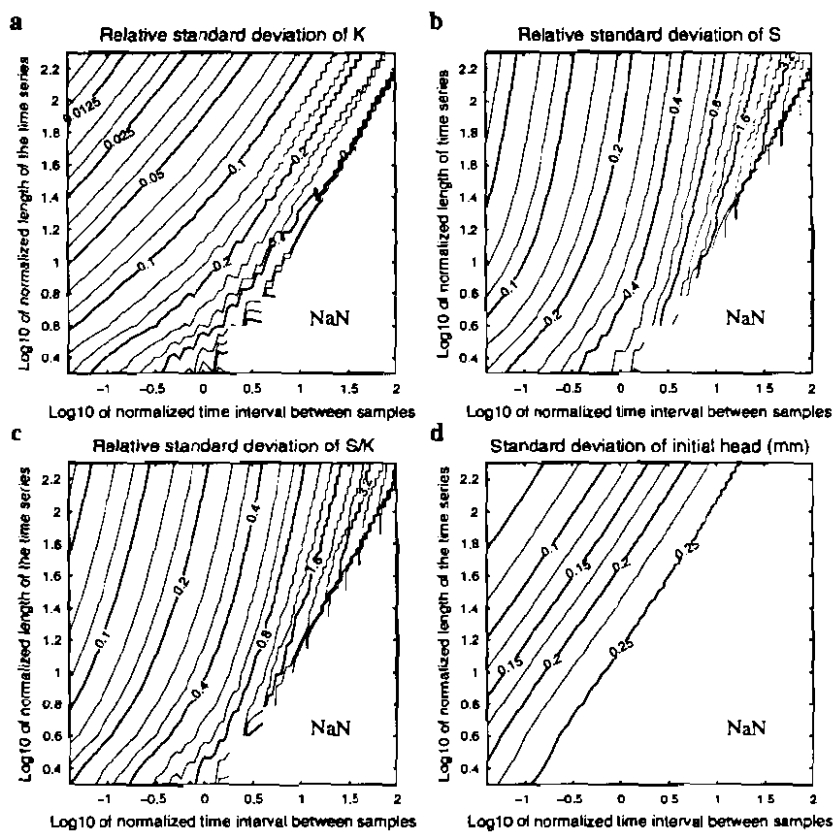


**Fig. 3.** Standard deviation of the model parameter as a function of the time interval between samples and the length of the time series. The x-axis is in time constants of  $\log_{10}(\Delta t/u)$  and the y-axis is in time constants of  $\log_{10}(t/u)$ , where  $u = Sr^2/4K$ , (cf. eq. 1). **a** is the relative standard deviation of  $K$ , **b** is the relative standard deviation of  $S$ , **c** is the relative standard deviation of  $S/K$ , and **d** is the standard deviation of the initial head.

**Field Example**

To evaluate practically the implementation of the method, preliminary field measurements have been carried out in Stjær gravel pit, East Jutland, Denmark. This location was chosen because of the expected homogeneity of the formation. Prior to the hydraulic log an electrical log and a gammalog were made (fig. 4e-f), using the Ellog Auger Drilling Method (Sørensen, 1989; Auken et al., 1994). Hydraulic measurements were carried out at six different depths in the phreatic aquifer. At each depth four injections were recorded, and for each injection the rise in potential head was measured at three distances from the injection source for both rising and decreasing potential corresponding to source-on and source-off. A separate inversion of the three distances and a joint inversion has been made on each hydraulic measurement, and the estimated hydraulic conductivities are shown in figure 4.

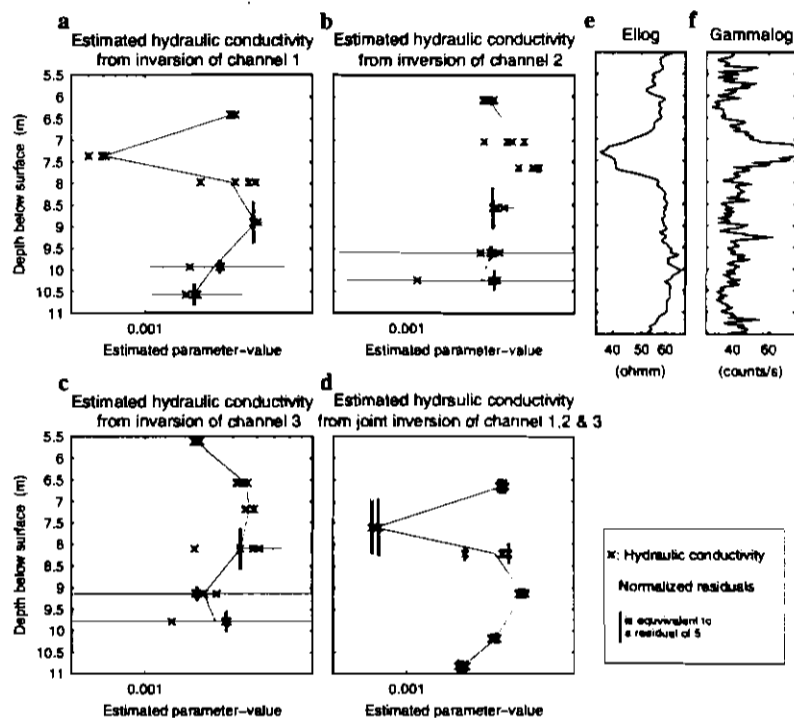


**Fig. 4.** a Estimated hydraulic conductivity from the inversion of channel 1, b channel 2, and c channel 3. The depth reference point is the midpoint of the configuration. d Estimated hydraulic conductivity from the joint inversion of channel 1, 2, and 3. The depth reference point is the depth of the source. Error bars are plotted as horizontal bars. The vertical bars are not error bars in depth but the normalized residuals (eq. 6). The residual scale is seen in the lower right corner. e Ellog and f Gammalog the depth scale is equal to the depth scale of the conductivity plots.

The ellog and gammalog show minor variations in the geology, which is also reflected in the injection log. A clayey layer is seen around 7.5 meters below the surface. At the same depth the hydraulic conductivity estimated from the inversion of the smallest spacing decreases. The central and largest spacing, however, show a minor increase in the conductivity, probably due to the large spacing compared to the thickness of the layer. The inconsistency between the three channels is reflected in the joint inversion as an increased normalized residual at the depth considered, i.e. at source depth of approximately 7.5 meters.

The variations between the estimated parameters at each depth are small, but not always within the estimated standard deviations (error bars) of the parameter estimates. This small variation indicates a high reproducibility.

The standard deviation of the model parameter estimates and the normalized residuals are generally small. However the normalized residual (eq. 6) of the joint inversion is large, around 3 in most cases. This must be attributed to the inconsistencies between the actual formation and the assumed model: the homogeneous and isotropic full space.

$$\text{Res} = \sqrt{\frac{1}{N} \sum_{i=1}^N \frac{(d_i - g(m_i))^2}{\sigma_{d_i}^2}} \quad (6)$$

A result of the joint inversion of the three channels at source depth 8.3 meters is shown in figure 5. The systematic deviation between the channels is probably (as mentioned above) caused by anisotropy, local inhomogeneities or local unknown conditions along the drill stem. The use of more spacings, both individually and joint, permits an estimation of the homogeneity of the formation and more spacings is equivalent to repeated experiments.

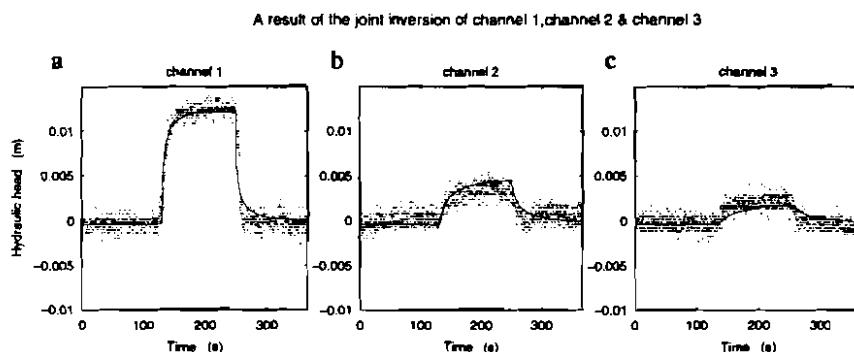


Fig. 5. An example of the result of the inversion on field data. The depth of the source is 8.3 meters below the surface. The dots are the measured data, the line is the response of the final model after inversion, a  $r = 0.5$  m, b  $r = 1.16$  m, c  $r = 2.085$  m.

The source which is assumed to be a step source may very well not be so. A gradually increasing source, would result in a smoother rise in the pressure data.



This would either cause an over estimation of the specific storage or it would introduce an inconsistency between the assumed model response and the actual response.

If instead a linear increasing source is used, it is possible to model the smooth rise in data (fig. 6). This means that another parameter, the run-on time, i.e. the time it takes for the source to reach a constant flow rate, must either be implemented in the model parameter space - in which case it must be expected to be tightly coupled to the specific storage - or accurately specified from additional independent measurements of the flow rate.

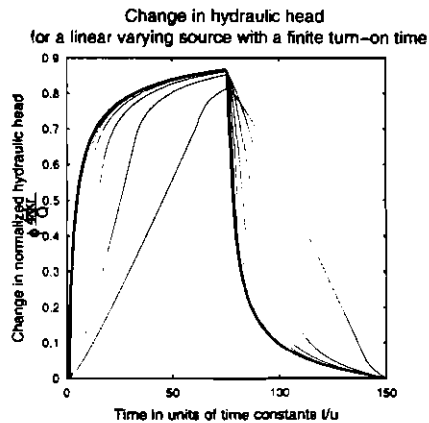


Fig. 6. Theoretical curves for a linear increasing source with finite turn-on times at: 2, 4, 8, 16, 32 and 64 time constants (eq. 8).

This implies that it is most essential to know the source function. In case of a varying source the resulting changes in the hydraulic head can be calculated employing the principle of superposition:

$$\phi(t, r) = \sum_{i=1}^N (Q_i - Q_{i-1}) \cdot \phi_0(t - t_i, r) \quad (7)$$

In case of linear variation in  $Q$  the difference  $Q' = Q_i - Q_{i-1}$  is constant for constant time steps  $\Delta t = t_i - t_{i-1}$ .  $Q'$  can then be isolated outside the summation and in the boundary where  $\Delta t$  approaches zero the sum converge towards the integral (fig 6):

$$\phi(t, r) = Q' \int_{t-\Delta}^t \phi_0(t - \tau, r) d\tau \quad (8)$$

### Conclusion and future work

This method for in situ determination of the hydraulic parameters is an attractive alternative to the slug test and a good supplement to the pumping test. As appears

from the analysis, it is possible to determine the hydraulic conductivity, but more difficult to determine the specific storage. Analysis of the inverse problem stresses the importance of dense measurements and, if possible, repeated experiments. Dense measurements together with strict control of the injection at early stages are most essential if the specific storage is needed. Analysis of the standard deviation of the model parameters, as a function of the model parameters  $K$  (hydraulic conductivity) and  $S$  (specific storage), show that the parameter standard deviation, in addition to the data noise and the injection,  $Q$ , mainly depends on the  $K$ -value. To get a satisfying determination of both  $K$  and  $S$  it is necessary to sample with a density of ten samples per characteristic time constant, whereas a time series length of only ten time constants should be sufficient. It is more efficient to make repeated measurements than just measure for a longer period. Due to inconsistency in data at an early stage, however, it is necessary to measure beyond ten time constants, and it is of primary importance to know the source function. The minimum length of the time series should be 30 time constants corresponding to approximately 80 % of the stationary level. It is also essential to measure before the injection is started to get information about the initial level.

Before further measurements are carried out the transducer system need to be improved. The assumption of the uncorrelated data is of course a presumption which should also be investigated in the future. Owing to air- or filter-resistance data might be correlated, although this correlation is expected to be small. Furthermore data processing, by means of a robust averaging, must take place in the field and finally a better control of the source is desirable.

More field measurements are planned in the near future, taking into account the experimental design resulting from this analysis.

### Acknowledgement

We would like to thank Bo Holm Jacobsen for valuable advice, and we would also like to thank Kent Sørensen for the work he has done on the development of the equipment and the collection of the data from Stjær.

### References

- Auken, E., Christensen, N. B., Sørensen, K. I., Effersø, F., 1994, Large scale hydrogeological investigation in the Beder area. Proceedings of the Symposium on the Application of Geophysics to Engineering and Environmental Problems, Boston, March 1994, pp. 615-628

- Carslaw, H. S., Jaeger, J. C., 1959. Conduction of heat in solids, Oxford University Press., pp. 195
- Charlez, Ph., Herail, R., Despax, D., 1989, Interpretation of Hydraulic Fracture Parameters by Inversion of Pressure Curves. *Int. J. Rock Mech. Min. Sci. & Geomech. Abstr.* Vol. 26, No. 6 pp. 549-553
- Fejes, I. and J6sa, E., 1990, The engineering geophysical sounding method: principles, instrumentation, and computerized interpretation, in Ward, Stanley H., Ed., *Geotechnical and environmental geophysics, 2: Soc. Expl. Geophys.*, pp. 321-331.
- Jacobsen, B. H., 1992, Nonlinear model construction and error propagation analyses: When does linearization work? *Proceedings of the Interdisciplinary Inversion Workshop 1*, pp. 63-68
- Jacobsen, B. H., 1993, Practical methods of a priori covariance specification for geophysical inversion. *Proceedings of the interdisciplinary Inversion Workshop 2*, pp. 1-10
- Menke, W., 1989, *Geophysical Data Analysis: Discrete Inverse Theory*. Academic Press. pp. 285
- Nielsen, S. B., 1992, Least squares inversion applied to thermal and hydrocarbon modelling. *Proceedings of the Interdisciplinary Inversion Workshop 1*, pp. 35-44
- Sørensen, K. I., 1989, A method for measuring the electrical formations resistivity while auger drilling, *First Break*, Vol. 7, No. 10, pp. 403-407.
- Sørensen, K. I., 1994, The Ellog Auger Drilling Method. *Proceedings of the Symposium on the Application of Geophysics to Engineering and Environmental problems*, Boston. March 1994, pp. 985-994
- Tarantola, A. and Valette, B., 1982, Generalized nonlinear inverse problems solved using the least squares criterion. *Reviews of Geophysics and Space Physics*. vol. 20, No. 2. pp. 219-232